

# Optimal Delay Compensation in Networked Predictive Control

Severin Beger \* Yihui Lin \* Katarina Stanojevic \*\*  
Sandra Hirche \*

\* Technical University of Munich (TUM), Munich, 80333 Germany  
(e-mail: {severin.beger}, {yihui.lin}, {hirche}@tum.de).

\*\* Technical University of Graz, Graz, 8010 Österreich (e-mail:  
katarina.stanojevic@tugraz.at)

**Abstract:** Networked Predictive Control is widely used to mitigate the effect of delays and dropouts in Networked Control Systems, particularly when these exceed the sampling time. A key design choice of these methods is the delay bound, which determines the prediction horizon and the robustness to information loss. This work develops a systematic method to select the optimal bound by quantifying the trade-off between prediction errors and open-loop operation caused by communication losses. Simulation studies demonstrate the performance gains achieved with the optimal bound.

**Keywords:** Control over Networks, Control under Communication Constraints, Remote Control, Delay Compensation, Networked Predictive Control, Model Predictive Control

## 1. INTRODUCTION

Modern control architectures rely increasingly on remote controllers and computations performed away from the plant. Examples include learning-based controllers that require substantial computational resources, as well as mobile and aerial robotic systems that offload control to cloud and edge infrastructures. While such networked control systems (NCS) offer many advantages, e.g., additional computational power, reduced energy and weight requirements on board, and flexible reconfiguration, they are subject to communication-induced constraints (cf. Zhang et al. (2020)). In particular, control over wireless all-purpose networks, such as WiFi (cf. Pezzutto et al. (2024)) or 5G, exhibits round-trip times (RTT) larger than the sampling period, together with non-negligible packet losses. These effects fundamentally challenge the design of stable and high-performance feedback controllers.

Strategies using predictive control methods for delay and dropout compensation, commonly referred to as networked predictive control (NPC), have received considerable attention over the last two decades. In an early work Bemporad (1998) established the idea of forwarding the input sequences of a remote model predictive controller (MPC) to the actuator in order to counteract large delays. Several subsequent works focus on pure delay compensation through prediction, such as Tang and de Silva (2006) and Liu et al. (2007), while others explicitly address dropouts due to communication, as seen in Quevedo et al. (2007) and Pezzutto et al. (2022).

Grüne et al. (2009) pointed out the importance of *prediction consistency*, i.e., ensuring that the controller's state predictions are based on the same inputs that are ultimately applied at the plant, when considering both delays and dropouts. Violations of prediction consistency may lead to infeasibility of the underlying optimal control prob-

lem and, in the worst case, to instability. Approaches guaranteeing prediction consistency include event-triggered or structure-preserving formulations, as in Varutti and Findeisen (2011) and Pin and Parisini (2011). Additionally, the inherent robustness of NPC schemes has been investigated by Findeisen et al. (2011).

Recently, the NPC paradigm has been extended to scenarios with completely unacknowledged (User Datagram Protocol (UDP)-like) communication in systems without time synchronization, considering time-varying delays and dropouts in both the uplink (plant-to-controller) and downlink (controller-to-plant) directions. Pin et al. (2021) ensure consistency through a move-blocking strategy, whereas Beger and Hirche (2024) introduce a two-mode architecture that distinguishes nominal operation from recovery after detected inconsistencies. Although these methods differ in several aspects, they share a crucial mechanism: the communication channel is represented by a fixed, deterministic delay bound  $\bar{\tau}$ . The controller computes inputs for a state predicted ahead for  $\bar{\tau}$  steps and discards all packets arriving later than  $\bar{\tau}$ , effectively interpreting excessive delays as dropouts.

The choice of  $\bar{\tau}$  is typically made conservatively, based on known bounds on delay and successive dropouts, or on engineering heuristics; yet, it has a direct and significant impact on closed-loop performance. A large bound increases prediction errors due to long forward roll-outs during prediction, while a small bound induces frequent dropouts and extended recovery phases from prediction inconsistencies. To the best of our knowledge, existing NPC schemes do not provide a systematic method for selecting  $\bar{\tau}$ , despite its central role in the compensation mechanism.

The contribution of this paper is two-fold. First, we develop a performance metric that quantitatively captures the trade-off between prediction errors during nominal

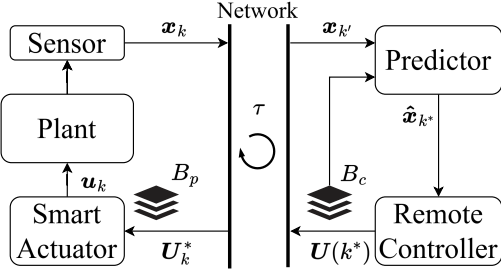


Fig. 1. Considered setup. The local controller forwards measurements to the remote side and receives actuation signals from the controller over a lossy network.

operation and recovery-related errors due to late or lost packets, explicitly as a function of the chosen delay bound and of the RTT distribution. Second, we show that this metric admits a minimiser, yielding an optimal delay bound  $\bar{\tau}^*$  for a given discrete delay distribution. The result provides a principled method for selecting the delay bound used in prediction-consistent NPC.

We structure the work as follows. In Section 2, we outline the system and assumptions on the communication network. The NPC algorithm under consideration is introduced in Section 3, followed by an error analysis in Section 4. This leads to our main result in Section 5, where we propose a method for selecting the optimal delay bound. Simulation studies in Section 6 demonstrate the effectiveness of the proposed approach. Finally, we conclude the work in Section 7.

## 2. SETUP AND PROBLEM STATEMENT

Consider a plant with discrete-time, linear time-invariant (LTI) dynamics subject to additive noise

$$\mathbf{x}_{k+1} = \mathbf{A}\mathbf{x}_k + \mathbf{B}\mathbf{u}_k + \mathbf{w}_k \quad (1)$$

where  $\mathbf{x}_k \in \mathbb{R}^n$  is the system state,  $\mathbf{u}_k \in \mathbb{R}^m$  is the control input, and  $\mathbf{w}_k \in \mathbb{W} \subseteq \mathbb{R}^n$  is an unknown, yet bounded additive disturbance with scalar bound  $\bar{w}$ . Furthermore, the plant is subject to state and input constraints, i.e.,  $\mathbf{x}_k \in \mathbb{X}, \mathbf{u}_k \in \mathbb{U}, \forall k$ , with  $\mathbb{U}, \mathbb{X}$  representing convex admissible sets. Additionally, we assume full state feedback and the uniform sampling period  $T_d$ .

*Remark 1.* (Continuous Time). In the following, we only discuss time in a discrete sense. Continuous time can always be recovered by multiplying the discrete time steps with the sampling period, i.e.  $t = k \cdot T_d$ .

The system is connected to a remote controller over a non-acknowledged, UDP-like packet-based communication network, cf. Fig. 1. All communication is subject to time-varying delays longer than a sampling step and packet losses. To characterise RTT delays  $\tau \in \mathbb{N}$ , all measurement packets from the sensor to the controller are time-stamped. The RTT represents the time from issuing a measurement packet at the sensor up until a controller message based on said measurement arrives back at the plant. Thus, it includes delays from the sensor-to-controller  $\tau_{sc} \in \mathbb{N}$ , the computation of new control values  $\tau_c \in \mathbb{N}$  and delays from controller-to-actuator  $\tau_{ca} \in \mathbb{N}$ . Furthermore, the following assumptions on the network hold:

*Assumption 2.1.* All RTT delays are independent and identically distributed (i.i.d.) according to the known

discrete delay distribution  $\mathcal{P}_\tau$ , i.e.  $p^\tau \sim \mathcal{P}_\tau$  with  $p_k^\tau = \Pr(p^\tau = k), k \in \mathbb{N}$ ,  $F(i) = \sum_{k=0}^i p_k^\tau$ .

*Remark 2.* (On the i.i.d. Delay Assumption). While real communication networks can exhibit temporal correlation, e.g., bursts of congestion or link-quality variations, this assumption is common in the design of NCS and provides a tractable baseline for analysis. For the proposed optimisation in this work, the key requirement is the ability to compute the per-step dropout probability and the distribution of repeated failures.

*Assumption 2.2.* The actuator and sensor are either collocated or synchronised and therefore operate on a common clock. The controller, in contrast, is not synchronised with the plant side so that no global clock alignment is required, preserving the flexibility of the networked architecture.

From Assumption 2.2 it follows that the RTT can be determined using the time stamp information, whereas the individual delays within the loop remain unknown.

NPC schemes have shown great potential for control over unreliable communication channels. A crucial parameter in these methods is the delay bound  $\bar{\tau}$ , which determines how far the controller predicts ahead and, thereby, the maximum delay that can be compensated. The aim of this paper is to develop a systematic method for selecting  $\bar{\tau}$  based on the RTT delay distribution. In the following, we first describe the NPC strategy, providing the structural and algorithmic framework required for the error analysis given in Section 4.

## 3. NETWORKED PREDICTIVE CONTROL STRATEGY

The core idea of NPC methods is to predict future states from past measurements and previously computed inputs with a constant delay bound  $\bar{\tau}$ , compute control sequences for these predicted states, and buffer them at the plant until their activation time arrives. This renders time-varying delay channels as constant delay  $\bar{\tau}$  and compensates for it at the downside of introducing artificial delay due to buffering. If values have RTT delays longer than  $\bar{\tau}$ , they are considered dropouts. Thus, with given delay probability distribution  $\mathcal{P}_\tau$ , the dropout probability for a given choice of  $\bar{\tau}$  is defined as

$$p_d(\bar{\tau}) = 1 - F(\bar{\tau}). \quad (2)$$

Dropouts can be compensated for by sending input sequences rather than single values, and then buffering these sequences and iterating them at the plant, should the next sequence not arrive in time. This is known as sequence forwarding. In addition to the network assumptions, we need to assume sufficient computational capabilities at the plant side to buffer newly arrived inputs, apply the decision logic required to select the appropriate control input from the buffered signals for the current time and to apply a simple fallback control law in case of long communication loss. In this paper, we adopt the NPC method from Beger and Hirche (2024) for delay and dropout compensation. Nevertheless, the reasoning of this work can be adapted to other known NPC methods, e.g. from Grüne et al. (2009) or Pin et al. (2021). We describe the considered method in the following in the necessary detail for the work at hand. When a new, delayed state measurement  $\mathbf{x}_{k'}$  measured

at time  $k'$  arrives at the controller side, the controller predicts the state  $\hat{\mathbf{x}}_{k^*}$  at a time  $k^* = k' + \bar{\tau}$  by rolling out the dynamics of the nominal model, i.e. (1) without considering  $\mathbf{w}_k$  as

$$\hat{\mathbf{x}}_{k^*} = \mathbf{A}^{\bar{\tau}} \mathbf{x}_{k'} + \sum_{i=0}^{\bar{\tau}-1} \mathbf{A}^{\bar{\tau}-i-1} \mathbf{B} \mathbf{u}_i \quad (3)$$

using previously calculated control inputs  $\mathbf{u}_i$  stored in the controller buffer  $B_c$ . The constant value  $\bar{\tau}$  represents the RTT bound, chosen a priori. It determines the number of steps for prediction and, therefore, the maximum delay that can be compensated. Based on the predicted future state  $\hat{\mathbf{x}}_{k^*}$ , an MPC input sequence  $\mathbf{U}(k^*) = [\mathbf{u}(0), \mathbf{u}(1), \dots, \mathbf{u}(N-1)]$  is computed by solving the optimal control problem (OCP)

$$\mathbb{P}(\hat{\mathbf{x}}_{k^*}) = \begin{cases} \min_{\mathbf{U}} \sum_{i=0}^{N-1} (\mathbf{x}_i^T \mathbf{Q} \mathbf{x}_i + \mathbf{u}_i^T \mathbf{R} \mathbf{u}_i) + \mathbf{x}_N^T \mathbf{P} \mathbf{x}_N \\ \text{s.t. } \mathbf{x}_i \in \mathbb{X}, \mathbf{u}_i \in \mathbb{U}, \mathbf{x}_N \in \mathbb{X}_N, \\ \mathbf{x}_{i+1} = \mathbf{A} \mathbf{x}_i + \mathbf{B} \mathbf{u}_i, \\ \mathbf{x}_0 = \hat{\mathbf{x}}_{k^*} \end{cases} \quad (4)$$

for a time horizon  $N$ , with a quadratic objective, where  $\mathbf{Q}, \mathbf{P} \succeq 0$  and  $\mathbf{R} \succ 0$ , denoting positive semi-definite and positive definite matrices, respectively. The system is subject to state and input constraints  $\mathbf{x}_k \in \mathbb{X}$  and  $\mathbf{u}_k \in \mathbb{U}$ . Furthermore, a terminal constraint set  $\mathbb{X}_N$  is considered that guarantees stability for a fallback control law

$$\mathbf{u}_k = \kappa(\mathbf{x}_k), \quad (5)$$

which is only in effect if too many consecutive packet dropouts prevent control inputs from reaching the plant. The resulting input sequence  $\mathbf{U}(k^*)$ , intended for application at time  $k^*$ , is buffered at the controller and transmitted to the plant. The plant maintains a buffer  $B_p$  of candidate input sequences satisfying  $k^* \geq k$ . In each step, the logic unit determines the best input sequence  $\mathbf{U}_k^*$  for the current time step. It first checks for a valid input sequence for the current time instant  $k$  in the buffer:  $\exists \mathbf{U}(k^*) \in B_p$  s.t.  $k^* = k$ . If such a sequence is available and it is predicted consistently in the sense of Grüne et al. (2009), the first value of it is applied. If no suitable sequence is available (because the packet was delayed beyond  $\bar{\tau}$  or lost), the plant reuses the previously applied input sequence  $\mathbf{U}_k^* = \mathbf{U}_{k-1}^*$  and advances to the next unused element within that sequence. This results in  $\mathbf{u}_k = \mathbf{u}(k - k^*) \in \mathbf{U}_k^*$  for  $k \leq N-1$ , and  $\mathbf{u}_k = \kappa(\mathbf{x}_k)$  once all values in the buffered sequence have been exhausted. While reusing previously applied control sequences maintains closed-loop operation during isolated packet delays or losses, it also introduces a critical vulnerability: the controller may continue predicting future states using input values that were never actually applied at the plant. In such a case, the predicted state used in (3) no longer reflects the true plant evolution, causing the controller's internal model to drift away from reality. This loss of prediction consistency (cf. Grüne et al. (2009)) prevents the controller from constructing a correct initial condition for the OCP (4), which leads to significant divergence from the optimal inputs and may eventually render the OCP infeasible. To guarantee prediction consistency, each input sequence carries a unique identifier. The controller compares the identifier reported in the next received measurement with the one used for its prediction. A mismatch

signals that the plant has reused outdated sequences. In this case, the algorithm enters *recovery mode*, where the controller repeatedly sends sequences based on the last consistent prediction until a successful error correction is reported back from the plant.

At the plant we discriminate two phases in the recovery mode: i) *Correction Phase*: After discarding a packet due to inconsistency the plant reuses the last consistent input sequence in open-loop until a correction input sequence from the controller arrives; ii) *Acknowledgement Phase*: Since all messaging in the network is considered to be unacknowledged, the plant needs to inform the controller of a successful error correction. It does this by adding a flag to the measurement packets once a correcting input sequence has arrived. Only then will the remote controller transition back to *nominal mode*. This phase causes the plant to run the successful correcting input sequence in open-loop, until the controller has transitioned back to nominal and a corresponding input sequence arrives at the plant. Therefore, the recovery mechanism ensures that prediction consistency is re-established whenever the network induces delays or dropouts that violate the nominal timing assumptions.

*Remark 3.* (Robustness Extension). In this work, only the logic component of the method from Beger and Hirche (2024) is considered, while the robustness aspect is omitted but can be readily incorporated into the proposed setup. As the system operates in a nominal and a recovery mode under unacknowledged communication, we need to discriminate 5 different system states as: ( $S_1$ ): Nominal mode for plant and controller; ( $S_2$ ): Correction mode for plant, nominal for controller; ( $S_3$ ): Correction mode for plant and controller; ( $S_4$ ): Acknowledgment mode for plant, correction for controller; ( $S_5$ ): Acknowledgment mode for plant, nominal for controller. Transitions proceed sequentially through these states. The only exception is state  $S_5$ : after the error recovery has been acknowledged, the system either returns to  $S_1$  if the next input sequence is received on time at the plant or transitions directly to  $S_2$  if the next packet is lost. Furthermore, since moving from one mode to the other requires a successful transmission at uplink or downlink in the network, we can model the behaviour between states with a Markov chain described by  $\pi_{k+1} = \pi_k \mathbf{P}(p_d)$  and its transition matrix

$$\mathbf{P}(p_d) = \begin{bmatrix} 1 - p_d & p_d & 0 & 0 & 0 \\ 0 & p_d & 1 - p_d & 0 & 0 \\ 0 & 0 & p_d & 1 - p_d & 0 \\ 0 & 0 & 0 & p_d & 1 - p_d \\ 1 - p_d & p_d & 0 & 0 & 0 \end{bmatrix}, \quad (6)$$

which may be analysed for stationary behaviour by using  $\lim_{k \rightarrow \infty} \pi_k = \pi_k \mathbf{P}(p_d)$ . The probability ratios of being in each of the states are given as

$$\begin{aligned} \pi_1 &= \frac{(1 - p_d)^2}{2p_d + 1}, & \pi_2 &= \pi_3 = \pi_4 = \frac{p_d}{2p_d + 1}, \\ \pi_5 &= \frac{p_d(1 - p_d)}{2p_d + 1}. \end{aligned} \quad (7)$$

As only plant states are considered, the weights are

$$\rho_1 = \pi_1, \quad \rho_2 = \pi_2 + \pi_3, \quad \rho_3 = \pi_4 + \pi_5. \quad (8)$$

*Remark 4.* (Up-/Downlink Delay Distribution). Since we only consider the RTT distribution  $\mathcal{P}_\tau$  to be known, we bound the uplink and downlink delay probabilities with  $\mathcal{P}_\tau$

whenever necessary in this work. The approach can be readily extended with distinct channel probabilities.

The choice of  $\bar{\tau}$  directly influences how often the system operates in each of the modes described above. A large  $\bar{\tau}$  reduces the likelihood of entering recovery but increases prediction errors due to longer forward rollouts in (3). Conversely, a small  $\bar{\tau}$  yields more frequent dropouts and thus causes transitions through the recovery and acknowledgement modes, accumulating additional correction-related errors. Since the stationary mode ratios in (7) determine how strongly each error type contributes to the long-term closed-loop behaviour, identifying the optimal delay bound requires a quantitative characterisation of the errors incurred in all modes, which is proposed in the following section. This enables the construction of an aggregate performance metric whose minimiser yields the optimal delay bound  $\bar{\tau}^*$ .

#### 4. ERROR TRADE-OFF IN NPC

In this section, a quantitative performance characterisation for the NPC scheme described in Section 3 is developed. To this end, we bound the expected worst-case state deviations stemming from predicting into the future, which leads to suboptimal control due to process noise, as well as the deviations from correcting the control behaviour from an inconsistent prediction, and from acknowledging the correction. Essentially, we analyse the resulting bounded and thus scalar errors of three distinct phases at the plant: nominal, error correction and acknowledgement.

The considered NPC scheme causes errors due to mismatches between the predicted state and the actual state at the time of application of a computed input value. We denote these state errors as  $e_k = \mathbf{x}_k - \hat{\mathbf{x}}_k$ . Considering (1), the error propagates as  $e_{k+1} = \mathbf{A}e_k + \mathbf{B}\Delta\mathbf{u}_k + \mathbf{w}_k$  where  $\Delta\mathbf{u}_k = \mathbf{u}_k - \hat{\mathbf{u}}_k$  represents the error between the actual applied input  $\mathbf{u}_k$  and the ideal predicted input  $\hat{\mathbf{u}}_k$  for that time. In the remainder of this work, we use the symbol  $\epsilon$  to denote scalar error values, bounded through a metric of choice.

##### 4.1 Fundamental Errors: Rollouts and Open-Loop-Behavior

To determine the optimal choice for the delay bound  $\bar{\tau}^*$ , we express the expected worst-case errors caused in the different modes of the NPC as functions of the delay bound  $\bar{\tau}$ . For the nominal mode, we introduce the error bound  $\epsilon_n(\bar{\tau})$ . In case of the recovery mode, we differentiate between the correction phase and the acknowledgement phase, resulting in error bounds  $\epsilon_c(\bar{\tau})$  and  $\epsilon_a(\bar{\tau})$ . All of these error bounds originate from two fundamental sources: (i) rollout errors, resulting from predicting the future state from a delayed measurement using the previously applied inputs, and (ii) open-loop errors, arising when the plant must temporarily reuse previously computed inputs. Firstly, due to the fact that the scheme ensures prediction consistency, the inputs used during prediction in the nominal mode are indeed the ones applied at the actuator, i.e.  $\Delta\mathbf{u}_k = \mathbf{0}$  holds. Thus, the difference between the actual state and the predicted state purely comes from propagating an initial state error alongside the unknown disturbances. It can be bounded by  $\|e_{k+1}\| \leq \|\mathbf{A}\| \|e_k\| + \bar{w}$ . We formulate the iterative error bound due to rollouts as

$$E_r(l, \epsilon_0) = \|\mathbf{A}\|^l \epsilon_0 + \bar{w} \sum_{i=0}^{l-1} \|\mathbf{A}^i\|, \quad (9)$$

where  $l$  is the number of steps rolling out the dynamics, and  $\epsilon_0 = \|e_0\|$  is the initial error bound. Secondly, open-loop errors occur when the plant must reuse an input sequence multiple times. This occurs when either no new input sequence is sent for a specific actuation time or when a dropout and subsequent prediction inconsistency result in an error recovery scenario. Under these circumstances, we need to bound the resulting input mismatch. In the case of a linear MPC, it can be bounded using a Lipschitz constant (cf. Teichrib and Darup (2023)) as  $\|\Delta\mathbf{u}_k\| \leq L\|\mathbf{e}_k\|$ . Bounding the error dynamics and plugging the Lipschitz bound in leads to  $\|\mathbf{e}_{k+1}\| \leq \Lambda\|\mathbf{e}_k\| + \bar{w}$  with  $\Lambda = \|\mathbf{A}\| + \|\mathbf{B}\|L$ . Thus, the iterative open-loop error bound can be written as

$$E_o^{(1)}(l, \epsilon_0) = \Lambda^l \epsilon_0 + \bar{w} \sum_{i=0}^{l-1} \Lambda^i, \quad \forall l < N_u, \quad (10)$$

where  $l$  is the number of consecutive steps reusing the same input sequence,  $\epsilon_0 = \|e_0\|$  represents a known initial error bound, and  $N_u$  is the number of available inputs left in the sequence. Additionally, the input sequence may run out of input values before new data arrives, requiring the definition of a second open-loop error component. In this case, the resulting input mismatch can be conservatively bounded as  $\|\kappa(\mathbf{x}_k) - \hat{\mathbf{u}}_k\| \leq 2\|\mathbf{B}\|\bar{u}$ , using the maximum bound of the inputs  $\bar{u}$ . This yields  $E_o^{(2)}(l, \epsilon_0) = \|\mathbf{A}^{l-N}\| E_o^{(1)}(N-1, \epsilon_0) + (\bar{w} + 2\|\mathbf{B}\|\bar{u}) \sum_{i=0}^{l-1} \|\mathbf{A}^i\|, \forall l \geq N_u$ . Combined, they give the piecewise open-loop error

$$E_o(l, \epsilon_0) = \begin{cases} E_o^{(1)}(l, \epsilon_0) & \text{if } l < N_u \\ E_o^{(2)}(l, \epsilon_0) & \text{if } l \geq N_u. \end{cases} \quad (11)$$

With the state roll-out error (9) and the open-loop error (11) at hand, we may now define the resulting errors of each plant side phase. We will drop the initial error bound  $\epsilon_0$  in the following for brevity whenever it is zero.

##### 4.2 Expected Error in Nominal Mode

The error at the plant from nominally predicted inputs is twofold. First, we need to consider an always-present error component  $E_r(\bar{\tau})$  due to simple rollouts for predicting the future state. Secondly, we may not trigger new computations of inputs due to packet disorder and thus, no new arrivals of control packets at the controller. This situation ultimately causes open-loop behaviour at the plant. Let  $T \in \mathbb{N}$  be a random variable denoting the number of additional steps for which the plant must reuse an old input sequence due to packet disorder. Then,  $\mathbb{E}(E_o(T, E_r(\bar{\tau}))) = \sum_{i=0}^{\infty} \Pr(T = i) E_o(i, E_r(\bar{\tau}))$  holds by the law of total expectation. In the following,  $\Pr(T = i)$  is characterised by considering two scenarios.

Firstly, an extension of  $i$  steps occurs if the next packet arrives  $i$  steps *earlier* than the previous one. This can only occur for  $i \leq \tau - 1$  steps. Let  $X_1, X_2 \sim \mathcal{P}_{\tau}$  denote independent packet delays. Then  $\Pr(T = i) = \Pr(X_2 - X_1 = -i) = p_{\Delta-}(i, \bar{\tau})$  holds. This can be explicitly computed as

$$p_{\Delta-}(i, \bar{\tau}) = \begin{cases} \sum_{k=0}^{\bar{\tau}-i} p_k^{\bar{\tau}} p_{k+i}^{\bar{\tau}}, & \text{if } i \in \{1, \dots, \bar{\tau}-1\} \\ 0 & \text{else.} \end{cases} \quad (12)$$

Secondly, an extension of length  $i$  due to *late* or *missing* packets occurs when a measurement packet with delay  $k$  is currently the most recent (probability  $p_k^f$  as in (14)) and no newer packet arrives in the next  $i$  steps, yielding

$$p_{\Delta+}(i, \bar{\tau}) = \sum_{k=0}^{\bar{\tau}} \left( p_k^f \prod_{j=k}^{k+i-1} (1 - F(j)) \right), \quad i \in \mathbb{N}_{>0} \quad (13)$$

$$\text{and } p_k^f = \frac{p_k^{\bar{\tau}} \prod_{r=0}^{k-1} (1 - p_r^{\bar{\tau}})}{1 - \prod_{r=0}^{\bar{\tau}} (1 - p_r^{\bar{\tau}})}. \quad (14)$$

All of the formulated components result in the expected nominal error

$$\epsilon_n(\bar{\tau}) = E_r(\bar{\tau}) + \sum_{i=1}^{\infty} (p_{\Delta-}(i, \bar{\tau}) + p_{\Delta+}(i, \bar{\tau})) E_o(i, E_r(\bar{\tau})). \quad (15)$$

As the sum of the probabilities of both disorder events individually is  $\leq 1$ , the series in (15) is absolutely convergent. When an inconsistent prediction occurs, the system enters recovery mode, which requires an error correction phase and, under a UPD-type network, an acknowledgement phase. We bound the errors for these phases in the following.

#### 4.3 Expected Errors in Recovery Mode

When an inconsistency is detected at the plant, it will reuse the last applied input sequence until a correcting one is received. During this time, the plant is in open-loop, and respective errors accumulate. Similarly to the nominal error, we have an always-occurring error part due to the constant buffering for  $\bar{\tau}$  and potential additional steps, resulting from delays and dropouts when communicating an error to the controller and receiving a correction. Let  $T_c \in \mathbb{N}_0$  be the number of additional steps required to successfully correct a prediction inconsistency. Assume that a correction requires at least one full RTT  $\bar{\tau}$ . Then, let  $\epsilon_o(\bar{\tau}) = E_o(\bar{\tau}, \epsilon_n(\bar{\tau}))$  be the guaranteed error for one correction cycle and  $\Delta E_o(i, \bar{\tau}) = E_o(\bar{\tau} + i, \epsilon_n) - \epsilon_o(\bar{\tau})$  the additional error for every additional step in the correction phase. Assume both channel delays and, therefore, dropout probabilities are drawn from the RTT distribution  $\mathcal{P}_{\tau}$ . Then, the expected per-step error for correcting a prediction inconsistency satisfies

$$\epsilon_c(\bar{\tau}) = \frac{\epsilon_o(\bar{\tau})}{\bar{\tau}} + \sum_{i=1}^{\infty} p_c(i) \Delta E_o(i, \bar{\tau}) \quad (16)$$

with  $p_c(i) = \Pr(T_c = i)$  given as

$$p_c(i) = (1 - p_d(\bar{\tau}))^2 (i + 1) p_d(\bar{\tau})^i. \quad (17)$$

This can be derived as follows: A correction of a prediction inconsistency requires two independent successful transmissions, one uplink and one downlink. Let  $X_1, X_2 \sim \text{Geom}(1 - p_d(\bar{\tau})) - 1$  be the required numbers of repeated attempts for each direction. Then  $T_c = X_1 + X_2$  and  $\Pr(T_c = i) = p_c(i)$  both hold, with the latter relation given in (17). This is true, since, as two independent successful transmissions are required and each attempt succeeds with

probability  $1 - p_d(\bar{\tau})$ , the number of failed attempts before completion follows from a negative binomial distribution with shape parameter  $s = 2$ , denoting the number of dropouts observed before we have the second successful transmission. The additional error from the pending correction for  $i$  steps is given by  $\Delta E_o(i, \bar{\tau})$ . Applying the law of total expectation, we have

$$\epsilon_c(\bar{\tau}) = \mathbb{E}[E_o(\bar{\tau} + T_c)] = \frac{\epsilon_o(\bar{\tau})}{\bar{\tau}} + \sum_{i=1}^{\infty} \Pr(T_c = i) \Delta E_o(i, \bar{\tau})$$

for the per-step error, which matches (16). Once the error is corrected at the plant, the controller must be informed about the correction to resume its nominal behaviour. Until then, the controller continues to send out correction trajectories, and the system will be in open-loop for at least one whole round-trip time. When the controller switches back to nominal mode, the next message from the controller to the actuator either causes the plant to return to nominal or again enter the error state. Now, we can formulate the acknowledgement error similarly to the prediction error. Let  $T_a \in \mathbb{N}_0$  be the number of additional steps required to successfully acknowledge the arrival of a correcting input sequence, such that the controller returns to nominal behaviour. Assume that an acknowledgement requires at least one full RTT  $\bar{\tau}$ . Then, let  $\epsilon_a(\bar{\tau}) = E_a(\bar{\tau}, \epsilon_n(\bar{\tau}))$  be the guaranteed error for one acknowledgement cycle and  $\Delta E_a(i, \bar{\tau}) = E_a(\bar{\tau} + i, \epsilon_n) - \epsilon_a(\bar{\tau})$  the additional error for every further step. Assume uplink channel delays and, therefore, dropout probabilities are drawn from the RTT distribution  $\mathcal{P}_{\tau}$ . Then, the expected per-step error for acknowledging the correction of a prediction error satisfies

$$\epsilon_a(\bar{\tau}) = \frac{\epsilon_o(\bar{\tau})}{\bar{\tau}} + \sum_{i=1}^{\infty} p_a(i) \Delta E_o(i, \bar{\tau}) \quad (18)$$

with  $p_a(i) = \Pr(T_a = i)$  given as

$$p_a(i) = (1 - p_d(\bar{\tau})) p_d(\bar{\tau})^i. \quad (19)$$

The main difference from the correction error is that only an uplink reception is necessary. Let  $X_1 \sim \text{Geom}(1 - p_d(\bar{\tau})) - 1$  denote the required number of repeated uplink attempts. Then  $T_a = X_1$  and  $\Pr(T_a = i) = p_a(i)$ , both hold, as defined in (19), following from the considered dropout distribution of a geometric series minus one. Furthermore, the additional error from the pending acknowledgement for  $i$  steps is described by  $\Delta E_a(i, \bar{\tau})$ . Again, we may apply the law of total expectation, yielding (18).

## 5. OPTIMAL DELAY BOUNDS IN NPC

Combining these errors weighted by their expected fraction of time spent in each phase through the weights (8) gives the performance index

$$\epsilon(\bar{\tau}) = \rho_1(\bar{\tau}) \epsilon_n(\bar{\tau}) + \rho_2(\bar{\tau}) \epsilon_c(\bar{\tau}) + \rho_3(\bar{\tau}) \epsilon_a(\bar{\tau}), \quad (20)$$

where  $\epsilon_n(\bar{\tau})$  represents the error in the nominal mode weighted with its total runtime ratio  $\rho_1(\bar{\tau})$ , while the error caused by the recovery mode is split into the correction phase  $\epsilon_c(\bar{\tau})$  and the acknowledgement phase  $\epsilon_a(\bar{\tau})$  with their respective ratios of the total runtime  $\rho_2(\bar{\tau})$  and  $\rho_3(\bar{\tau})$ . This metric, in turn, can be minimized to find the optimal delay bound choice  $\bar{\tau}^*$  as

$$\bar{\tau}^* = \operatorname{argmin}_{\bar{\tau}} \epsilon(\bar{\tau}). \quad (21)$$

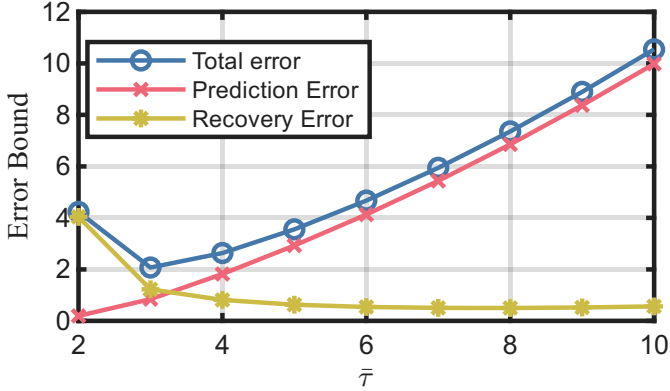


Fig. 2. The weighted errors in (20) with system (22) and a log-normal distribution with  $\mu = 0.5$  and  $\sigma = 0.5$  and input weighting  $\mathbf{R} = 1$  illustrating the trade-off between prediction and recovery errors. The resulting optimal delay bound is  $\bar{\tau}^* = 3$ .

For each  $\bar{\tau} \in \mathbb{N}$ , the performance index  $\epsilon(\bar{\tau})$  is well-defined, non-negative, and finite. Since the optimization domain is discrete and bounded by construction, a minimizing delay bound  $\bar{\tau}^*$  always exists.

The derived performance metric in (20) captures the trade-off between the expected errors occurring during nominal operation and those arising during recovery with respect to the chosen delay bound  $\bar{\tau}$ . Because  $\epsilon_n(\bar{\tau})$  grows with increasing  $\bar{\tau}$ , while  $\epsilon_c(\bar{\tau})$  and  $\epsilon_a(\bar{\tau})$  increase as  $\bar{\tau}$  decreases, the resulting performance index exhibits a unique minimum in all evaluated scenarios. Fig. 2 shows an exemplary sweep of (20) over a range of RTT delay bounds and highlights the discussed error trade-off.

In the next section, we demonstrate that considering the optimal delay bound  $\bar{\tau}^*$  yields higher performance than selecting an arbitrary constant value.

## 6. SIMULATION RESULTS

The performance of the proposed strategy is demonstrated in the following simulation study. We consider a mass-spring-damper system with dynamics

$$\dot{\mathbf{x}} = \begin{bmatrix} 0 & 1 \\ -k/m & -d/m \end{bmatrix} \mathbf{x} + \begin{bmatrix} 0 \\ 1/m \end{bmatrix} \mathbf{u} + \mathbf{w}_k, \quad (22)$$

where  $m = 1\text{kg}$ ,  $k = 10\frac{\text{N}}{\text{m}}$  and  $d = 0.5\frac{\text{Ns}}{\text{m}}$ . The states represent position  $x_1$  and velocity  $x_2$ , respectively. We choose a sampling time  $T_d = 50\text{ms}$  for discretisation and add white noise to the acceleration bounded by  $\bar{w} = 0.1\frac{\text{N}}{\text{kg}}$ . The chosen second-order system has a fairly low damping ratio of  $\zeta = d/(2\sqrt{km}) \approx 0.79$  and a natural frequency of  $\omega_0 = \sqrt{k/m} \approx 3.16\frac{1}{\text{s}}$ . In conjunction with the rather long sampling time, this makes the system sensitive to noise and thus to state errors due to open-loop behaviour caused by communication imperfections. The inputs are constrained as  $|\bar{u}| = 25\text{N}$ . With MPC weighting matrices  $\mathbf{Q} = \text{diag}(500, 1)$  and  $\mathbf{R} = 0.1$  we can approximate the global Lipschitz bound as  $L = 87.3$  through an explicit MPC method. All simulations are carried out in *Matlab/Simulink 2025b*, using the toolbox *NetFlex* from Stanojevic et al. (2025).

We sample all delays from log-normal distributions with

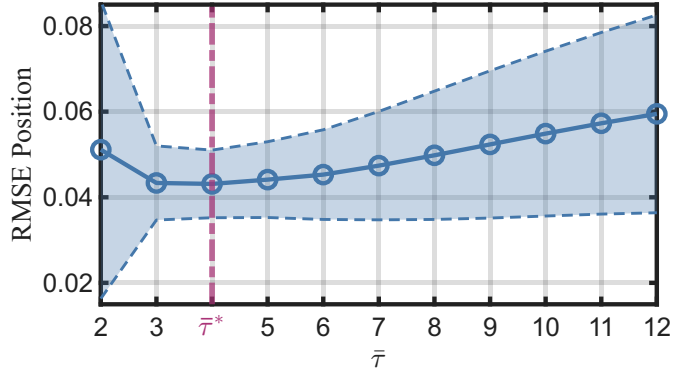


Fig. 3. A sweep of the position RMSE over several delays for the presented algorithm. The optimum aligns with the predicted value for  $\bar{\tau}^* = 4$ . A total of 100 runs were conducted.

parameters  $\mu$  and  $\sigma$ , and subsequently discretise them. These distributions possess heavy tails and resemble typical network delay behaviour. We then allocate the delay between the sensor-controller and controller-actuator channels by sampling a random split proportion  $p_s$  drawn from a beta distribution with parameters  $\alpha = \beta = 2$  and setting  $\tau_{sc,k} = \text{round}(p_s \tau_k)$  and  $\tau_{ca,k} = \tau_k - \tau_{sc,k}$ . This ensures that the simulated round-trip delays match the theoretical distribution, while allowing for variability and asymmetry between uplink and downlink delays.

*Remark 5.* (Infinite Dropouts). In numerical calculations, we replace the infinity bound as prevalent in (15), (16) and (18) with  $c_{\bar{\tau}} \in \mathbb{N}$ , which results from a probabilistic assumption such as  $(p_d(\bar{\tau}))^{\bar{\tau}+c_{\bar{\tau}}} < 0.001$ .

At first, we consider the delay distribution  $\mathcal{P}_{\bar{\tau}}^1$  as a log-normal distribution with  $\mu_1 = 0.5, \sigma_1 = 0.5$ , resulting in a mean delay of 3.1. Evaluating (21) leads to  $\bar{\tau}^* = 4$ . To evaluate performance, we apply two unit steps to the position reference at  $t = 0\text{s}$  and  $t = 3\text{s}$ , respectively and conduct 100 simulation runs. Each run sweeps over a set of potential delay bounds using the same delay distribution. The resulting RMSE position errors with their 95% confidence interval are depicted in Fig. 3. We observe that the optimally predicted delay bound lines up with the lowest average error, although adjacent values are not far off. This is to be expected, as the optimisation minimises the expected worst-case error. Importantly, the proposed bound is optimal in expectation and demonstrates the highest consistency, as seen by the minimal variance around its optimum.

In a second experiment with the same reference, we alter the delay distribution from  $\mathcal{P}_{\bar{\tau}}^1$  to  $\mathcal{P}_{\bar{\tau}}^2$  with  $\mu_2 = 1.5$  and  $\sigma_2 = 0.5$  at  $t = 3\text{s}$ . For each distribution, we compute the optimal time delay bound with (21) as  $\bar{\tau}_1^* = 4$  and  $\bar{\tau}_2^* = 7$  respectively. To assess performance, we conduct three different runs: the first two apply one of the optimal delay bounds for the entire duration, while the third run adapts the delay bound at the right time, thereby utilising the optimal delay bound at all times. We conducted this experiment 100 times, each with varying disturbances and resampled delays. Fig. 4 shows the resulting position over time, together with a 95% confidence interval depicted as shaded regions. The result indicates that the adaptive strategy outperforms the constant ones, suggesting that the optimal delay bound choice indeed leads to a per-

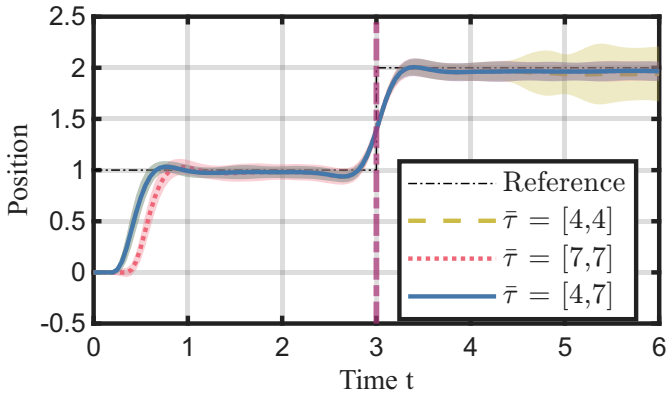


Fig. 4. Comparison of three runs with different assumed delay bounds tracking two successive step changes. The log-normal delay distribution is changed at  $t = 3s$  from  $\mu_1 = \sigma_1 = 0.5$  to  $\mu_2 = 1.5$  and  $\sigma_2 = 0.5$ .

formance increase and may be valuable as an adaptive strategy for online sampled delay distributions.

## 7. CONCLUSION

This work introduces a systematic method for determining the optimal delay bound  $\bar{\tau}^*$  in networked predictive control based on a known delay distribution  $\mathcal{P}_\tau$ . By decomposing the closed-loop behaviour into nominal, correction, and acknowledgment phases, we derived a performance metric (20) that captures the fundamental trade-off between prediction-induced errors and open-loop behaviour caused by packet dropouts. Minimizing this metric (21) yields the delay bound that optimizes expected closed-loop performance. In simulations, we have shown the effectiveness of the method. The proposed framework provides a principled design tool for NPC schemes and establishes a foundation for future work on correlated or time-varying delay models and online adaptation of the delay bound.

## DECLARATION OF GENERATIVE AI AND AI-ASSISTED TECHNOLOGIES IN THE WRITING PROCESS

During the preparation of this work, the authors utilized ChatGPT and Grammarly to enhance the writing and technical content. After using this tool, the authors reviewed and edited the content as needed and take full responsibility for the content of the publication.

## REFERENCES

Beger, S. and Hirche, S. (2024). A Robust Model Predictive Control Method for Networked Control Systems. In *2024 IEEE 63rd Conference on Decision and Control (CDC)*, 6896–6903.

Bemporad, A. (1998). Predictive control of teleoperated constrained systems with unbounded communication delays. In *Proceedings of the 37th IEEE Conference on Decision and Control*, 2133–2138 vol.2.

Findeisen, R., Grüne, L., Pannek, J., and Varutti, P. (2011). Robustness of Prediction Based Delay Compensation for Nonlinear Systems. *IFAC Proceedings Volumes*, 44(1), 203–208.

Grüne, L., Pannek, J., and Worthmann, K. (2009). A prediction based control scheme for networked systems with delays and packet dropouts. In *Proceedings of the 48th IEEE Conference on Decision and Control (CDC) held jointly with 2009 28th Chinese Control Conference*, 537–542.

Liu, G.P., Xia, Y., Chen, J., Rees, D., and Hu, W. (2007). Networked Predictive Control of Systems With Random Network Delays in Both Forward and Feedback Channels. *IEEE Transactions on Industrial Electronics*, 54(3), 1282–1297.

Pezzutto, M., Dey, S., Garone, E., Gatsis, K., Johansson, K.H., and Schenato, L. (2024). Wireless control: Retrospective and open vistas. *Annual Reviews in Control*, 58, 100972.

Pezzutto, M., Farina, M., Carli, R., and Schenato, L. (2022). Remote MPC for Tracking Over Lossy Networks. *IEEE Control Systems Letters*, 6, 1040–1045.

Pin, G., Fenu, G., Casagrande, V., Zorzenon, D., and Parisini, T. (2021). Robust Stabilization of a Class of Nonlinear Systems Controlled Over Communication Networks. *IEEE Transactions on Automatic Control*, 66(7), 3036–3051.

Pin, G. and Parisini, T. (2011). Networked Predictive Control of Uncertain Constrained Nonlinear Systems: Recursive Feasibility and Input-to-State Stability Analysis. *IEEE Transactions on Automatic Control*, 56(1), 72–87.

Quevedo, D., Silva E., and Goodwin G. (2007). Packetized Predictive Control over Erasure Channels. In *2007 American Control Conference*, 1003–1008.

Stanojevic, K., Steinberger, M., Siljak, M., Ludwiger, J., and Horn, M. (2025). NetFlex: A Simulation Framework for Networked Control Systems. In *IFAC 11th International Conference on Control, Decision and Information Technologies (CoDIT) 2025*.

Tang, P.L. and de Silva, C.W. (2006). Compensation for transmission delays in an ethernet-based control network using variable-horizon predictive control. *IEEE Transactions on Control Systems Technology*, 14(4), 707–718.

Teichrib, D. and Darup, M.S. (2023). Efficient Computation of Lipschitz Constants for MPC with Symmetries. In *2023 IEEE Conference on Decision and Control (CDC)*, 6685–6691.

Varutti, P. and Findeisen, R. (2011). Event-based NMPC for networked control systems over UDP-like communication channels. In *Proceedings of the 2011 American Control Conference*, 3166–3171.

Zhang, X.M., Han, Q.L., Ge, X., Ding, D., Ding, L., Yue. D., and Peng, C. (2020). Networked control systems: A survey of trends and techniques. *IEEE/CAA Journal of Automatica Sinica*, 7(1), 1–17.